Distribution and characters of the mud diapirs and mud volcanoes off southwest Taiwan

CrossMark

Song-Chuen Chen [a,b], Shu-Kun Hsu [a,*], Yunshuen Wang [b], San-Hsiung Chung [b], Po-Chun Chen [b], Ching-Hui Tsai [a], Char-Shine Liu [c], Hsiao-Shan Lin [a], Yuan-Wei Lee [d]

[a] Department of Earth Sciences, National Central University, Taiwan
[b] Central Geological Survey, Ministry of Economic Affairs, Taiwan
[c] Institute of Oceanography, National Taiwan University, Taiwan
[d] Exploration and Production Business Division, CPC Corporation, Taiwan

ARTICLE INFO

ABSTRACT

In order to identify the mud diapirs and mud volcanoes off SW Taiwan, we have examined ~1500 km long MCS profiles and related marine geophysical data. Our results show ten quasi-linear mud diapirs, oriented NNE–SSW to N–S directions. Thirteen mud volcanoes are identified from the multibeam bathymetric data. These mud volcanoes generally occur on tops of the diapiric structures. Moreover, the active mud flow tracks out of mud volcanoes MV1, MV3 and MV6 are observed through the high backscatter intensity stripes on the sidescan sonar images. The heights of the cone-shaped mud volcanoes range from 65 m to 345 m, and the diameters at base from 680 m to 4100 m. These mud volcanoes have abrupt slopes between 5.3° and 13.6°, implying the mudflow is active and highly viscous. In contrast, the flat crests of mud volcanoes are due to relative lower-viscosity flows. The larger cone-shaped mud volcanoes located at deeper water depths could be related to a longer eruption history. The formation of mud diapirs and volcanoes in the study area are ascribed to the overpressure in sedimentary layers, compressional tectonic forces and gas-bearing fluids. Especially, the gas-bearing fluid plays an important role in enhancing the intrusion after the diapirism as a large amount of gas expulsions is observed. The morphology of the upper Kaoping Slope is mainly controlled by mud diapiric intrusions.

© 2013 Elsevier Ltd. All rights reserved.

1. Introduction

A mud diapir is an intrusive structure characterized by a slowly upward migrating mass of clay-rich sediment and fluid discharge (Kopf, 2002). A mud volcano usually occurs above the diapir, as a result of fluid migration directly along the body of the mud diapir or through faults (fractures) connected to the mud diapirs (Milkov, 2000; Kopf, 2002). Cone-shaped mud volcanoes with central vents are common features (Brown, 1990; Kopf, 2002). Mud volcanoes represent the last manifestation of diapirism (Brown and Westbrook, 1988; Pérez-Belzuz et al., 1997; Kopf, 2002). They are the most important pathways for methane emission from deep marine sediments into atmosphere (Dimitrov, 2002, 2003). They have been studied intensively because they are closely related to the occurrence of hydrocarbons (e.g. gas hydrate) and fluid discharge (mainly methane and CO_2), an important component of global carbon cycles (Milkov, 2000; Kopf, 2002).

Mud volcanism and diapirism are well-known geological phenomena occurring in the areas of ongoing collisional tectonics or extensional settings. The majority occur in accretionary wedges, where the main tectonic forces are of compressional, such as in the Mediterranean Ridge (Limonov et al., 1996; Camerlenghi et al., 1995; Robertson et al., 1996; Kopf et al., 1998, 2000), Barbados (Brown and Westbrook, 1988; Sumner and Westbrook, 2001), Gulf of Cádiz (León et al., 2007; Somoza et al., 2003) and Nankai Trough (Kobayashi et al., 1992; Morita et al., 2004). Some occurs in extensional provinces, such as in the Black Sea (Krastel et al., 2003; Limonov et al., 1997) and Southeastern Tyrrhenian Sea (Gamberi and Rovere, 2010). Some mud diapirs and mud volcanoes have been linked to both extensive and compressive contexts, such as in the Western Alboran Sea area (Pérez-Belzuz et al., 1997; Sautkin et al., 2003; Talukder et al., 2003). In addition to high overpressure in sedimentary layers due to rapid sedimentation and gas generation (Dimitrov, 2002; Milkov, 2000; Talukder et al., 2007; Brown, 1990; Hovland and Curzi, 1989; Hovland et al., 1997), tectonic processes are considered to be the main driving mechanism for the development of mud diapirism and volcanism (Milkov, 2000; Talukder et al., 2007; Limonov et al., 1996).

The offshore area of SW Taiwan belongs to an accretionary wedge setting that is caused by the southeastward subduction of the Eurasian Plate beneath the Philippine Sea Plate. Many

submarine mud volcanoes, gas seeps and mud diapirs have been reported (Fig. 1) (Sun and Liu, 1993; Liu et al., 1997; Huang, 1995; Chang, 1993; Chuang, 2006; Tseng, 2006; Chiu et al., 2006; Lin et al., 2009; Chen et al., 2010; Hsu et al., 2013a,b). Onland mud volcanoes have also been documented in southern Taiwan (Shih, 1967; Yang et al., 2004; Sun et al., 2010). The formation of mud volcanoes onshore and offshore may be linked (Yeh, 2003; Yang et al., 2004; Sun et al., 2010). Some submarine diapiric ridges are also suggested to be structurally correlated with the similar anticlinal structures in SW Taiwan (Hsieh, 1970; Sun and Liu, 1993; Huang, 1995; Liu et al., 1997; Chuang, 2006). However,

due to lack of detailed marine geophysical data, the characteristics of the submarine structural features, mud volcanoes and diapirs are still poorly understood in the offshore area of SW Taiwan.

For the past six years, new marine geophysical data have been collected in the offshore area of SW Taiwan, giving a good opportunity to better understand the accurate distribution and characters of the mud diapirs and mud volcanoes. In this paper, we use the newly collected multibeam bathymetry, multichannel seismic reflection (MCS) and deep-towed sidescan sonar data to map the structures of the mud diapirs and mud volcanoes in the offshore area of SW Taiwan.
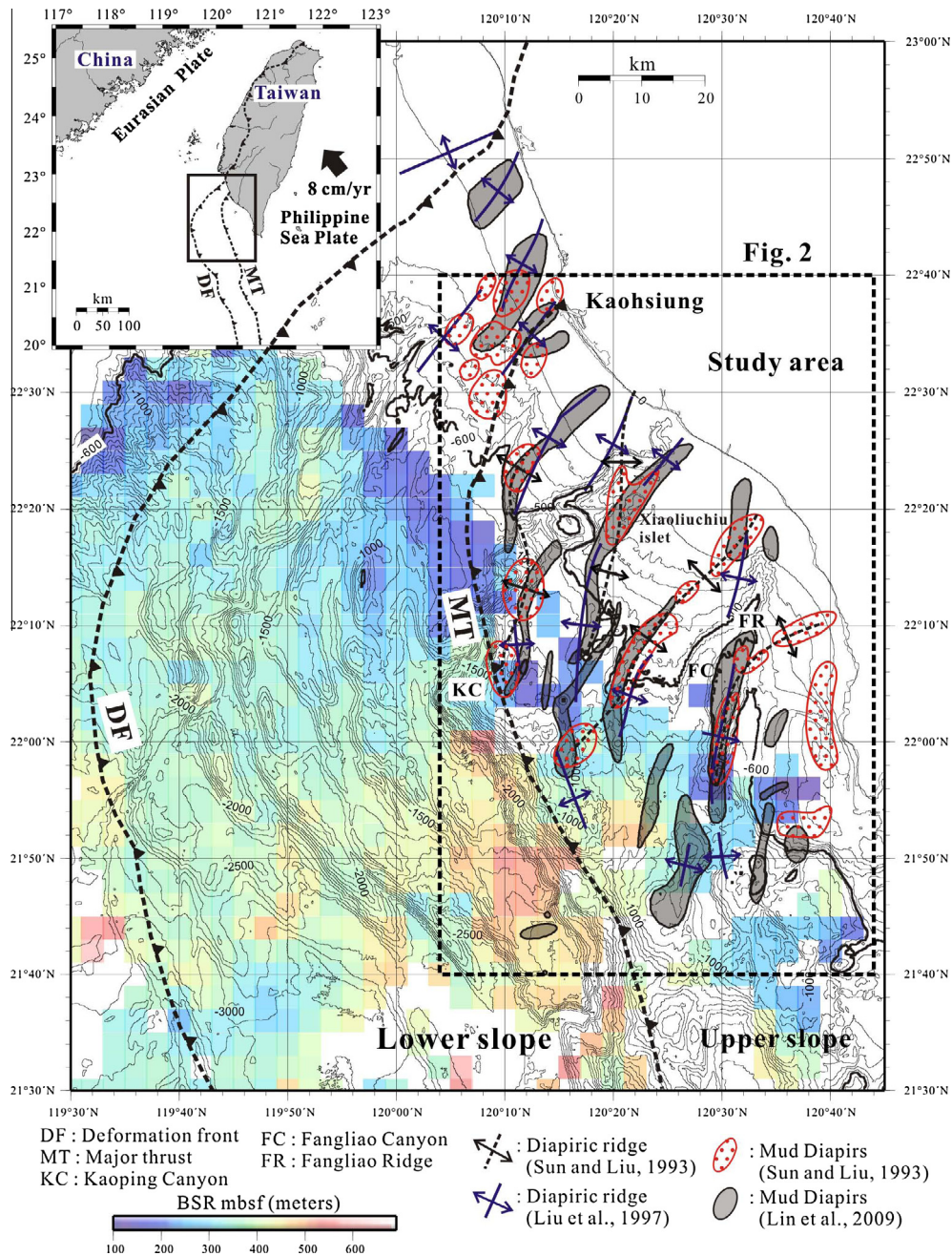
Fig. 1. Tectonic features and bathymetry off SW Taiwan. Inset shows the regional topography and tectonic features. The deformation front (DF) separates the passive South China Sea (SCS) continental margin in the west and active accretionary wedge in the east. The major thrust (MT) separates the lower slope and upper slope of the accretionary wedge. The different distributions of the mud diapirs or diapiric ridges off SW Taiwan are plotted for comparison. The dashed box indicates our study area. The distribution of the bottom simulating reflector (BSR) (in 2′ × 2′ grids) is indicated by the color scale. mbsf: meters below seafloor.

2. Geological background

Our study area is located in the offshore area of SW Taiwan, where the passive Chinese continental margin in the west encroaches on the western margin of the Taiwan mountain belt in the east (Reed et al., 1992; Liu et al., 1997, 2004). In between, the deformation front (DF) is the northward continuation of the Manila Trench to Taiwan (Fig. 1). Distinctive fold-and-thrust ridges occur to the east of the DF, while horst and graben structures occur to the west of the DF. The accretionary wedge can be divided into the upper and lower slope domains (Fig. 1) (Reed et al., 1992; Liu et al., 1997; Lin et al., 2008, 2009). The lower slope domain is characterized by a series of anticlinal ridges related to active thrusting and folding (Liu et al., 2004; Lin et al., 2008). In contrast, the upper slope domain is characterized by smooth seafloor topography and chaotic seismic structures, probably due to deeply dipping beds and intense deformation (Liu et al., 2006; Lin et al., 2008, 2009). The lower slope domain is more active in terms of thrusting and folding; in contrast, the upper slope domain is marked by gas venting, mud volcanoes and diapiric structures (Sun and Liu, 1993; Chiu et al., 2006; Chuang, 2006; Chen et al., 2010).

3. Method and data

Multibeam bathymetric data were collected in 2010 by using the multibeam echo sounder Altas MD50 system operated at a frequency of 50 kHz onboard R/V OR2. The multibeam echo sounder Kongsberg EM710 and EM302 systems, operated at frequency ranges 76–100 kHz and 26–34 kHz, also surveyed the mud volcano area onboard M/V POLARIS in 2011. All the data were post-processed and displayed with the softwares of CARAIBES and GMT, respectively.

In this study, we use 39 MCS profiles with a total length of ~1500 km. The MCS profiles were collected with a high-resolution multichannel seismic data acquisition system during the cruises MCS-793, MCS-928, MCS2-1616 and MGL-0908 (Fig. 2). Among the profiles, MCS-793, MCS-928 and MCS2-1616 profiles have a total length of ~1344 km and were collected by using 24, 12 and 12 channels with streamer length of 300 m, 75 m and 75 m were collected onboard R/V OR1, OR1 and OR2 in 2006, 2007 and 2009, respectively. The MGL-0908 profiles have a total length of ~156 km and were collected in 2009 by using 468 channels with a streamer length of 6000 m onboard R/V Marcus G. Langseth. All the MCS profiles were processed by using PROMAX interactive seismic processing software.

The deep-towed sidescan sonar data were collected onboard R/V OR1 in 2009. Profiles SBP-Line 1 and Line 8, having a total length of ~22 km, are used in the study (Fig. 3). The towing speed during the survey was between 2.0–3.0 knots and the tow-fish was kept at 30–50 m above the seafloor. The sidescan sonar is dual frequency at 120 kHz and 410 kHz. The 120 kHz and 410 kHz modes provide across-track resolutions of 6.25 cm and 1.9 cm, respectively. The chirp sub-bottom profiler operates at 1–6 kHz, giving a vertical resolution of 15–25 cm. The position of the tow-fish was calculated by a layback using the ship's GPS position, the bathymetric profile recorded beneath the ship and the bathymetric profile recorded beneath the tow-fish.

4. Results

Based on the multichannel seismic reflection (MCS) profiles and multibeam bathymetric data, we have identified ten mud diapir structures (MD1 to MD10) and thirteen mud volcanoes (MV1 to MV13) in the study area (Figs. 2 and 3). In general, the mud volcanoes are distributed on tops of the mud diapirs, implying that the formation of the mud volcanoes is directly associated with the mud diapirism.

A bottom simulating reflector (BSR) identified from a seismic reflection profile is attributed to the presence of gas hydrate above the BSR in the sedimentary strata or ample free gas accumulated beneath the BSR (Holbrook et al., 1996; Hyndman and Dallimore, 2001; Liu et al., 2006; Bangs et al., 2005). In our study area, the BSRs have been identified on MCS profiles MGL-0908-0 and 0908-1A (Figs. 4 and 5). The strong acoustic contrast of the reflections at the BSR and high-amplitude reflections beneath the BSR are clearly observed in MCS profile MGL-0908-0 (Fig. 4). It suggests the presence of gas hydrate above the BSR and/or a free gas accumulation beneath the gas hydrate-bearing sedimentary layer. In any case, the ample free gas can provide a strong source for the formation of mud diapirs and mud volcanoes off SW Taiwan.

4.1. Mud diapirs

Mud diapirs can be recognized on seismic profile in terms of acoustically amorphous piercement structures (Sun and Liu, 1993; Liu et al., 1997). The sedimentary strata on both sides of a mud diapir exhibit onlapping structures due to the uplifting of the diapir.

We have identified ten mud diapiric structures, MD1 to MD10, distributed in the near shore area of SW Taiwan (Fig. 2). The distribution of the mud diapirs is somewhat different from the mud diapirs documented in previous studies (Fig. 1). For instance, MD1 extends more northward and reaches the near-shore area; MD2 extends southwestward and does not shift to the south direction; MD3 consists of two branches of diapiric intrusions; MD4 is defined for the first time; MD5, MD6 and MD7 are longer.

Our new identified mud diapirs are in NNE–SSW to N–S orientation (Fig. 2). The lengths of the mud diapiric ridges are from 3.9 to 56.5 km and the widths are from 1.6 to 8.3 km. The maximum length of the mud diapiric ridges are longer than the ones in the Barbados accretionary complex (Brown and Westbrook, 1988) and in the Western Alboran Sea (Pérez-Belzuz et al., 1997). Most of the diapiric structures are covered by a layer of young sediments, but some have pierced through sediments and are exposed at the seafloor, such as the Shell-Tomb Ridge and south pinnacle of diapir MD5, Fangliao Ridge (diapir MD8) and Xiaoliuchiu islet (diapir MD2) (Figs. 2 and 4–7).

Mud diapir MD1 is located along the eastern flank of the Kaoping (also named Gaoping) Canyon to the south of N22°18′ and along the western flank in the north of N22°18′ (Fig. 2). It can be clearly recognized on the MCS profiles (Figs. 6 and 7). Based on MCS profile MCS2-1616-1b (Fig. 7), mud diapir MD2 is located at the eastern flank of the Kaoping Canyon (Figs. 2 and 7). The canyon course developed along the flank of a diapir or between two diapirs, indicating that the canyon course is controlled by mud diapiric intrusions (Chiang and Yu, 2006; Yu et al., 2009). Mud diapirs MD1 and MD2 extend northward to the near shore and could be structurally correlated with the Fangshan and Pingtung anticlines in SW Taiwan, respectively (Fig. 2; Hsieh, 1970; Huang, 1995; Chuang, 2006). The Xiaoliuchiu islet is situated on diapir MD2 and has been uplifted above the sea level (Sun and Liu, 1993; Liu et al., 1997; Lacombe et al., 2004). The exposed diapiric mudstone in Xiaoliuchiu islet named as Xiaoliuchiu mudstone is the upper part of the diapiric formation in late Pliocene (Sun and Liu, 1993; Chi, 1981). The major uplifting of Xiaoliuchiu islet may have happened in Plio-Pleistocene due to compressional tectonic forces (Lacombe et al., 2004).

Compared to the other diapiric structures, the development of diapir MD3 is more complex. MD3 consists of two branches of the diapiric structure: MD3-1 and MD3-2 (Figs. 2 and 3). The structure of MD3-1 is separated from MD3 near mud volcano MV6
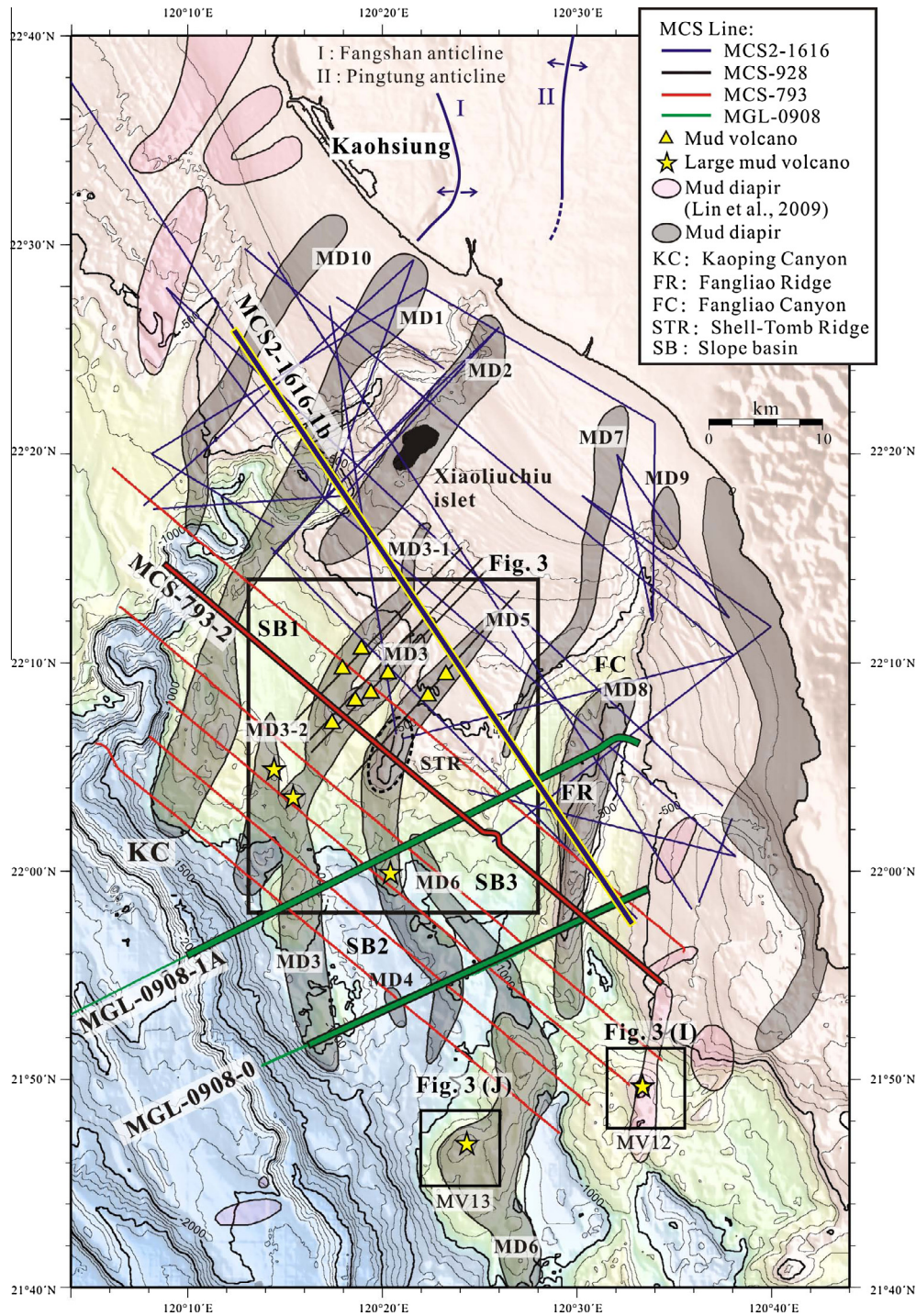
Fig. 2. Multibeam bathymetry and related structures of the study area. Ten mud diapirs (gray polygons) and thirteen mud volcanoes (yellow triangles and stars) are recognized on the basis of the MCS profiles and multibeam bathymetry. Five large mud volcanoes are indicated by yellow stars (diameters of 2800–4100 m). The solid black, blue, red and green lines are different MCS lines. (For interpretation of the references to color in this figure legend, the reader is referred to the web version of this article.)

(Fig. 3). The separation of MD3 and MD3-1 is shown in MCS-793-2 and MCS-793-1 (Fig. 8). In total, 8 mud volcanoes (MV3 to MV10) have developed on top of mud diapir MD3 (Figs. 2 and 3), demonstrating that MD3 has experienced vigorous fluid flow. In addition, sedimentary strata on both sides of diapir MD3 are disturbed and the diapir is almost exposed at the seafloor (covered only by thin sediments) (Figs. 4 and 5), indicating that MD3 is still growing.

MD4 is comparatively small. It appears within of the slope basin (SB2) between MD3 and MD5 (Figs. 2 and 4). It could be a young intrusion that occurred after the diapirism of MD3 and MD5. Despite the small area of MD4, it is clearly recognized in the MCS profile MGL-0908-0 (Fig. 4). The bottom simulating reflector (BSR) is well developed above MD4 and high-amplitude reflections are observed beneath the BSR (Fig. 4). It suggests the presence of gas hydrate above the BSR and free gas accumulation beneath
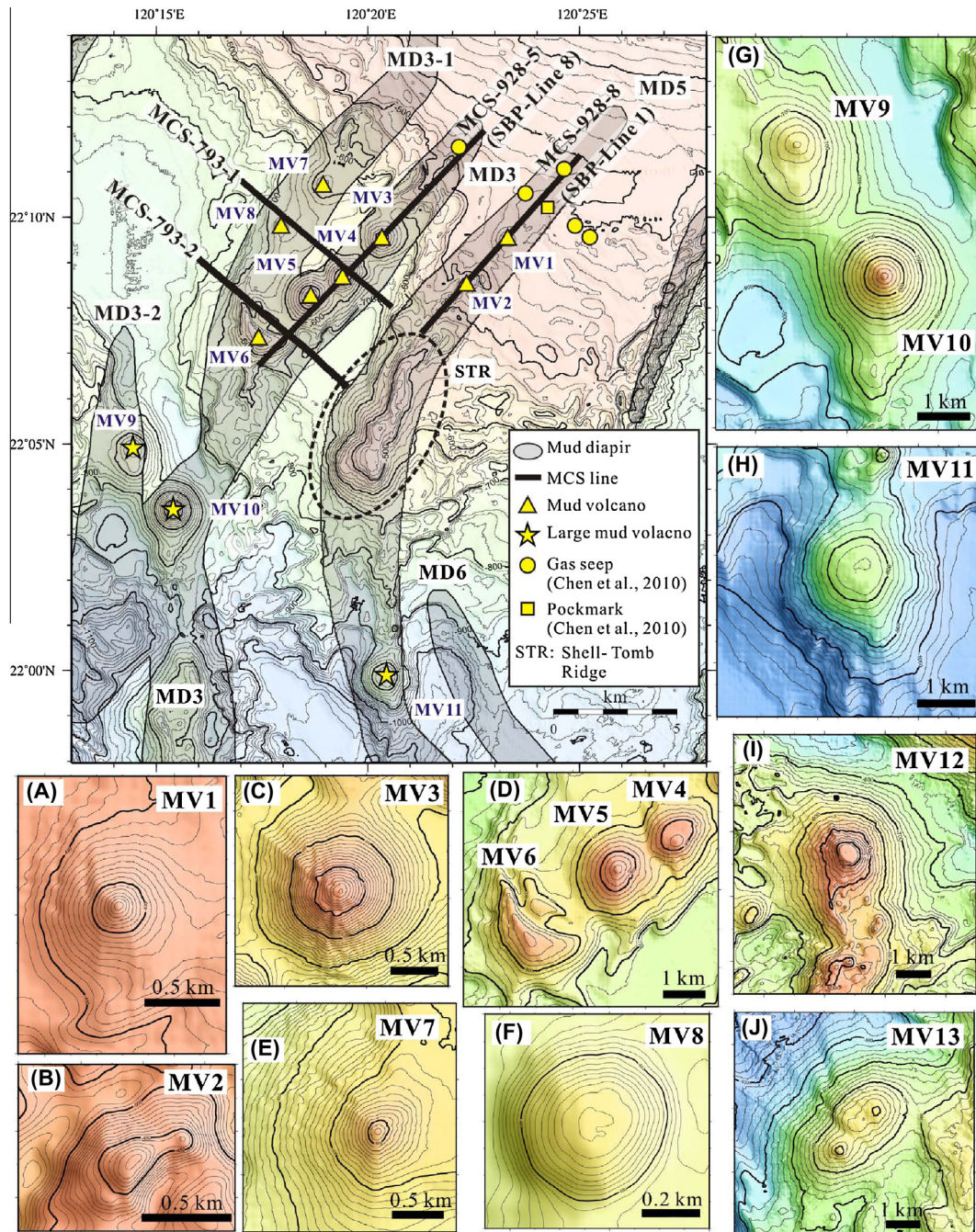
Fig. 3. The distribution of mud volcanoes and diapirs (see the location in Fig. 2). These mud volcanoes are situated on tops of the mud diapirs. Insets A to J are the detailed topography of the mud volcanoes. Mud volcanoes MV8, MV11 and MV12 show flat edifice on their crests, while the other mud volcanoes have steep cone-shaped craters. The location of mud volcanoes MV12 (I) and MV13 (J) are shown in Fig. 2.

the BSR. The fluid conduit is observed above the diapiric structure where a BSR is absent (Fig. 4), indicating that the gas comes from the diapiric structure and migrates upwards to a gas-hydrate–bearing sedimentary layer.

MD5 is located in the middle of the study area (Fig. 2). MV1, MV2, MV11 and the Shell-Tomb Ridge have developed from this diapiric structure (Fig. 3). Several gas seeps and one pockmark were reported in the northern end of MD5 and MD3 (Fig. 3) (Chen et al., 2010), also suggesting that the fluid of gas seeps comes from the diapiric structure. The Shell-Tomb Ridge is one of the diapiric structures and is exposed at the seafloor as shown in the MCS-793-2 (Fig. 6). The Shell-Tomb Ridge is characterized by

widely distributed shell fragments and carbonated crust on the seafloor (Chen et al., 2012). The south pinnacle of MD5 is exposed at the seafloor (Fig. 4), indicating that the diapir is still active.

MD6 is located between MD5 and MD8 (Fig. 2). Mud volcano MV13 has developed in the southern part of MD6. MD7 and MD9 are located at the both sides of the Fangliao Canyon head (Fig. 2), indicating that the development of the canyon course is constrained by the diapirs. The morphology of MD8 (Fangliao Ridge) shows a very steep slope and is one of the diapiric structures exposed at the seafloor (Fig. 2). The disturbance of sedimentary strata on the both sides of MD8 (Figs. 4–7) indicates that MD8 is also active. Mud diapir MD10 is located in the west of the Kaoping
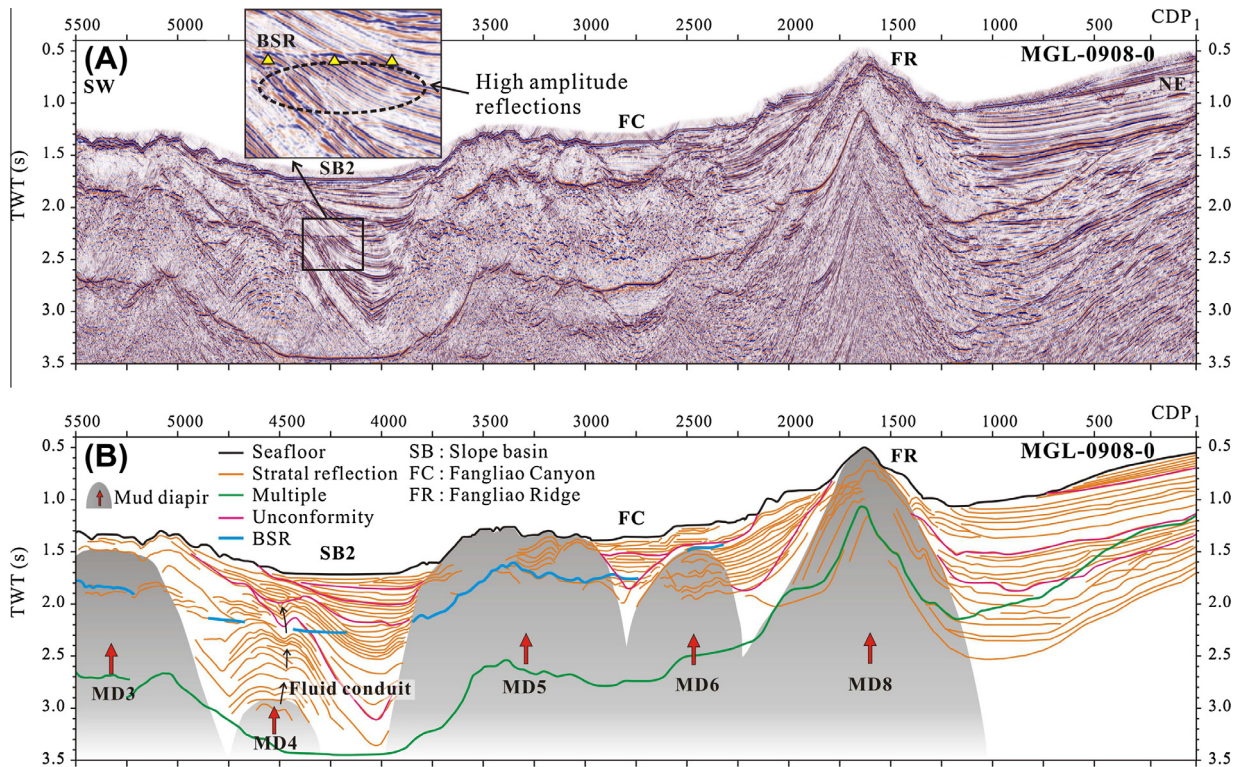
Fig. 4. (A) MCS profile and (B) the interpreted seismic profile of MGL-0908-0. Five mud diapirs are present in this profile. The mud diapirs MD8 (Fangliao Ridge) and MD5 have pierced through thick sediments and are exposed at the seafloor. Diapir MD4 has developed between diapirs MD3 and MD5. BSRs and high amplitude reflections beneath BSR are clearly observed in this profile. The slope basin SB2 is formed between the structural highs. See the profile location in Fig. 2.

Canyon (Fig. 2) and extends northward to the near shore. MD10 is probably inactive because its top is covered by a sedimentary layer (Fig. 7).

4.2. Mud volcanoes

On the basis of the multibeam bathymetry, 13 mud volcanoes (MV1 to MV13) are recognized in the study area (Figs. 2 and 3). These mud volcanoes are situated on tops of mud diapiric structures. The fluid source for the mud volcanoes probably comes from the associated diapiric structure and the fluid migrates upward along fractures to the seafloor.

The mud volcanoes are typically cone-shaped, except that MV6 is more elongated (Fig. 3). The heights of the mud volcanoes range from 65 m to 345 m and the diameters at base range from 680 m to 4100 m (Fig. 3; Table 1). These mud volcano sizes are quite similar to other mud volcanoes around the world, such as in the Barbados Ridge (Brown and Westbrook, 1988), in the Western Alboran Sea (Pérez-Belzuz et al., 1997), in the Black Sea (Krastel et al., 2003) and in the Eastern Nankai Trough (Morita et al., 2004). Additionally, the slopes of the mud volcanoes off SW Taiwan range from 5.3° to 13.6°, which are also consistent with the slopes of the mud volcanoes in the Black Sea (Krastel et al., 2003), in the Western Alboran Sea (Pérez-Belzuz et al., 1997) and in the Gulf of Cádiz (eastern Central Atlantic) (Somoza et al., 2003; León et al., 2007).

Two deep-towed sidescan sonar and sub-bottom profiler images (SBP-Line 1 and 8), and seismic profiles MCS-928-5 and MCS-928-8 (Figs. 3, 9 and 10) are used to better understand the characteristics of the seafloor and sub-seafloor at the area of mud volcanoes MV1 to MV6. Several gas seeps are identified based on the sub-bottom profiler images of SBP-Line 1 and Line 8 (Figs. 9 and 10). The stripes of radial high backscatter intensity (light tones) on the flanks of mud volcanoes MV1, MV3 and MV6 can be interpreted as mud flows (Figs. 9 and 10). The mud flow indi-

cates active eruptions. In mud volcano MV1, the radial mud flows edifice is clearly observed on the mosaic image of sidescan sonar data and by ROV observations (Fig. 11). High backscatter intensity is also observed on the flank of mud volcano MV2 (Fig. 9), which could be caused by rough relief of the mud flows. Additionally, the very high backscatter intensity spot in the center of MV1, MV2 and MV3 (Figs. 9 and 10) could be interpreted as the area of fluid and mud emission at the seafloor (Gamberi and Rovere, 2010). Alternatively, the high backscatter intensity in the center of a mud volcano could be due to a very irregular relief of the crater and cone (Limonov et al., 1997).

In a cold seep site, the authigenic carbonates, chemosynthetic communities or gas hydrate may cause rough seafloor. As well, the high acoustic impedance contrast may increase acoustic backscatter intensity of the sidescan sonar image (Orange et al., 2002; Johnson et al., 2003; Holland et al., 2006; Talukder et al., 2007; Naudts et al., 2008). Thus, we suggest that the high backscatter intensity in the south area of MV2 is due to the existence of chemosynthetic communities or authigenic carbonates on the seafloor (Fig. 9).

5. Discussion

5.1. Mud diapirism

We suggest three major mechanisms that generated the diapirism in our study area. Firstly, the overpressure in sedimentary layers is caused by a rapid sedimentation rate. Secondly, the mud diapirism is caused by the compressional tectonic forces. Thirdly, an ample discharge of gas-bearing fluids can increase the mud buoyancy to facilitate diapiric intrusion.

Mud diapirs are driven by buoyancy forces due to the bulk density contrast between an overpressured muddy mass and an
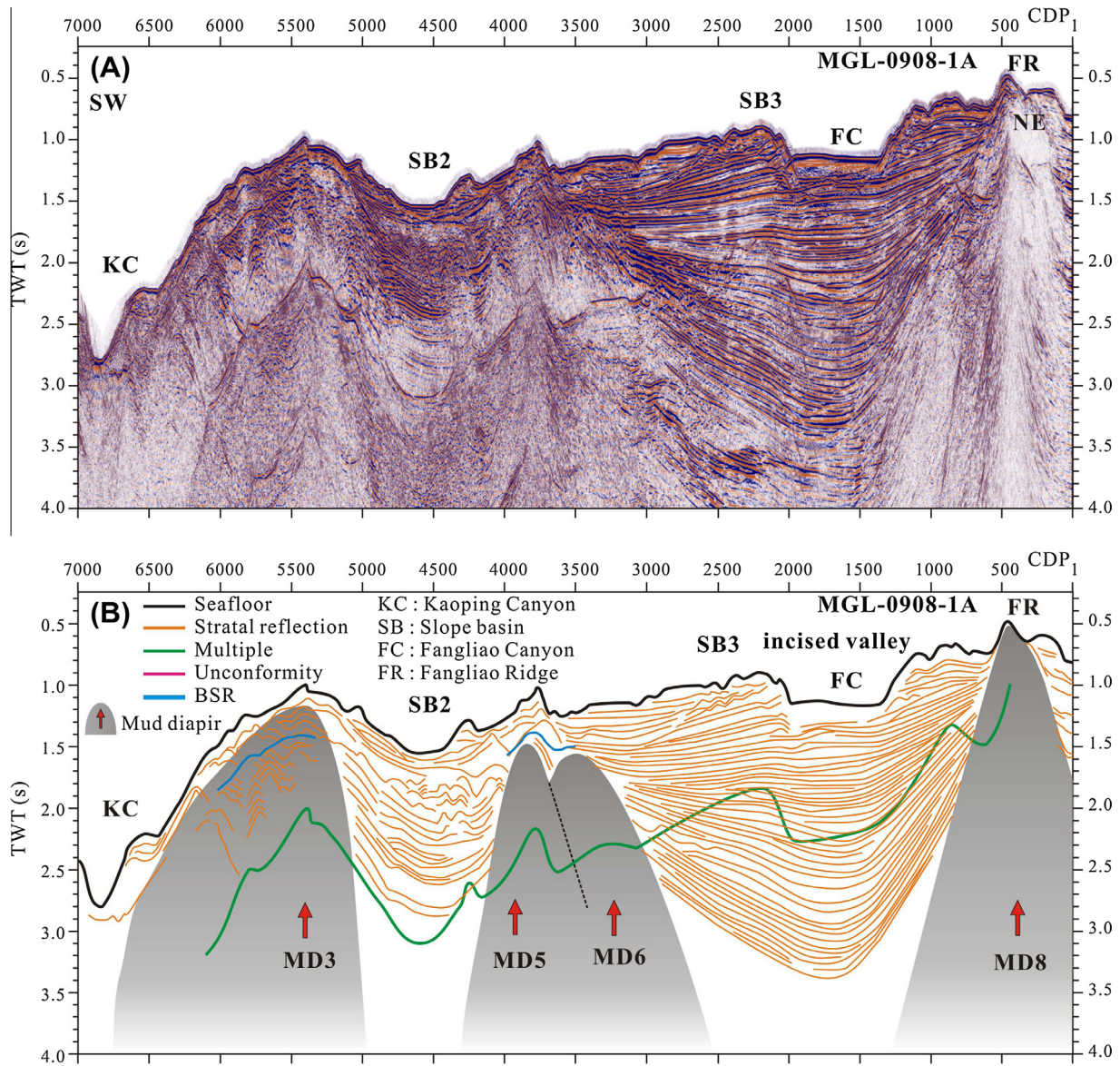
Fig. 5. (A) MCS profile and (B) the interpreted seismic profile of MGL-0908-1A. Four mud diapirs are present in this profile. Mud diapir MD8 (Fangliao Ridge) is exposed at the seafloor. BSRs are clearly observed in this profile. The slope basins SB2 and SB3 are formed between the structural highs. See the profile location in Fig. 2.

overburden of greater density (Brown, 1990). A rapid sedimentation rate is believed to be the main reason for overpressure in sedimentary layers (Milkov, 2000; Talukder et al., 2007). A rapid sedimentation rate results from a large amount of sediments from land, specifically from SW Taiwan which contributes ~49 Mt/yr suspended sediments (Dadson et al., 2003). The large amount of sediments is attributed to high erosion rates of 3–6 mm/yr, mainly due to heavy rainfall during frequent typhoons in Taiwan (Dadson et al., 2003), with an average of four typhoons per year. A large typhoon event can deposit a flood layer of ~3–10 cm off SW Taiwan (Hale et al., 2012), indicating that storms provide a first-order control on the erosion rate in Taiwan (Dadson et al., 2003). In SW Taiwan, the Kaoping River connected to Kaoping submarine canyon is a main sediment dispersal system, and most of sediments transported by Kaoping River through Kaoping Canyon are dispersed to the offshore area of SW Taiwan (Yu et al., 2009; Huh et al., 2009). In fact, rapid sedimentation rates from 0.7 to 4.5 mm/yr were estimated on the basis of ^{14}C dating data of foraminifera from

a giant piston core (~35.14 m long) in the accretionary wedge off SW Taiwan (Lin et al., 2013).

The distribution of these mud diapirs trends NNE–SSW to N–S, the same orientation as the structural features trends onland Taiwan that are formed by the Penglai orogeny in the Pliocene (Bowin et al., 1978; Ho, 1986; Teng, 1990). We suggest that the mud diapirism is caused by the compressional tectonic forces of the Penglai orogeny due to the similar orientations of structures onland and mud diapirs in the offshore.

Gas-charged sediments are regarded as an important factor in the diapir formation (Hovland and Curzi, 1989). The common presence of methane in mud volcanoes provides a driving force for hydrogeologic and intrusive systems because of voluminous quantities of fluid, decreasing mud densities and increasing buoyancy forces in diapirs (Brown, 1990). Methane is considered to play an important role in the mechanism of mud diapirism and volcanism (Brown, 1990; Hovland and Curzi, 1989). High methane concentrations have been observed in the water column above the mud volcanoes
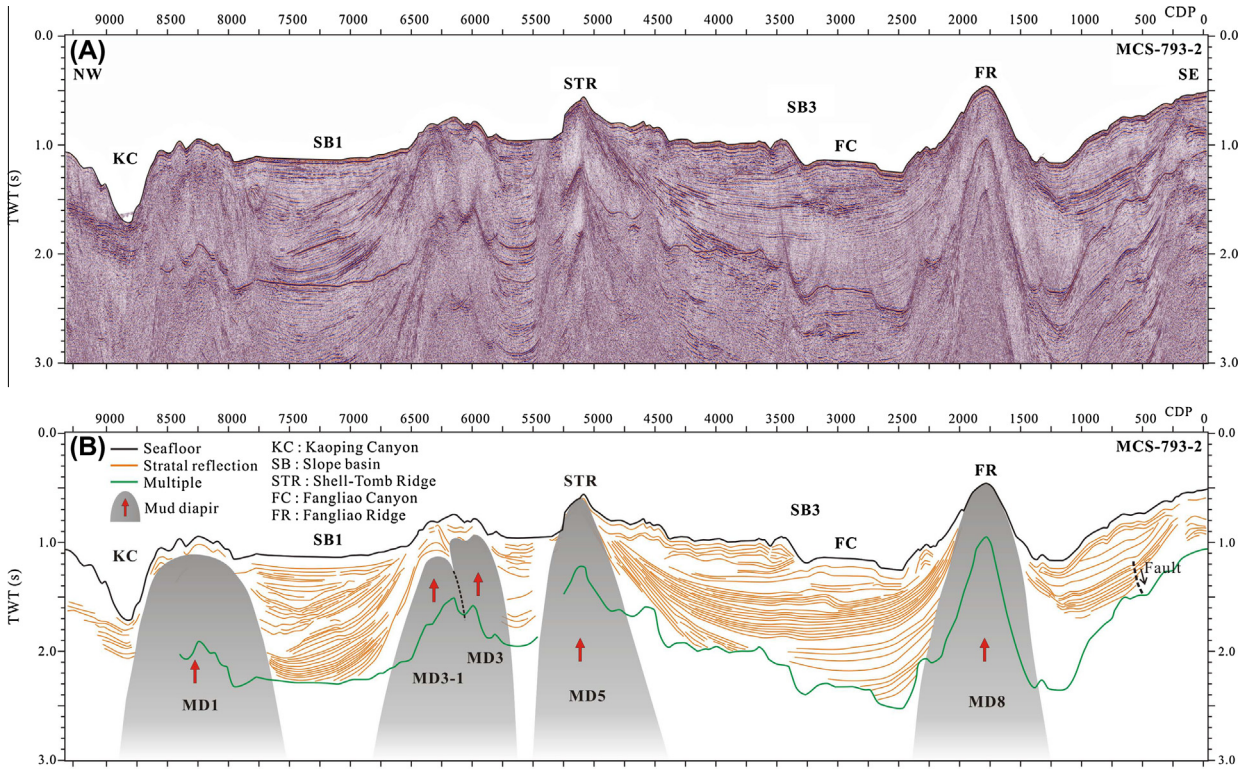
Fig. 6. (A) MCS profile and (B) the interpreted seismic profile of MCS-793-2. Five mud diapirs are present in this profile. Mud diapir MD8 (Fangliao Ridge) and Shell-Tomb Ridge have pierced through thick sediments and are exposed at the seafloor. The slope basins SB1 and SB3 are formed between the structural highs. See the profile location in Fig. 2.
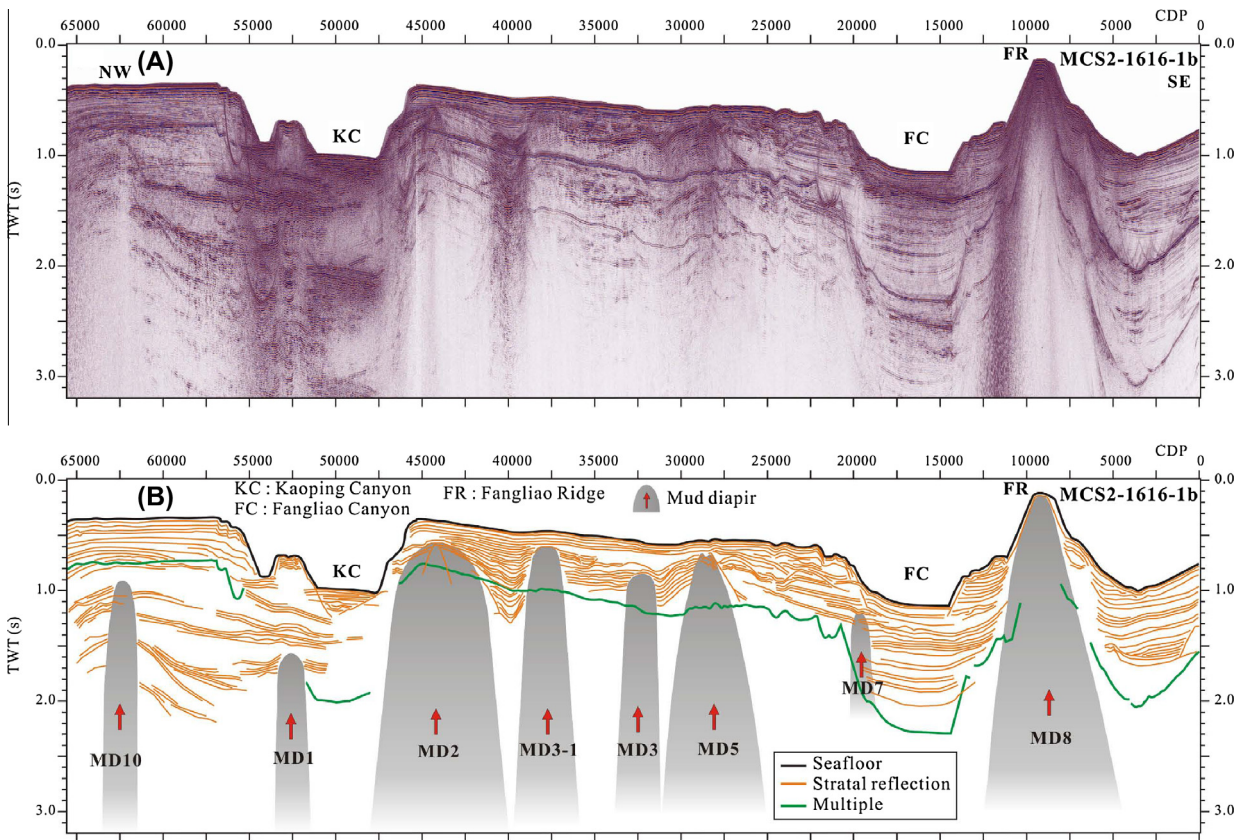
Fig. 7. (A) MCS profile and (B) the interpreted seismic profile of MCS2-1616-1b. Eight mud diapirs are present in this profile. The mud diapir MD8 (Fangliao Ridge) has pierced through thick sediments and is exposed at the seafloor. See the profile location in Fig. 2.
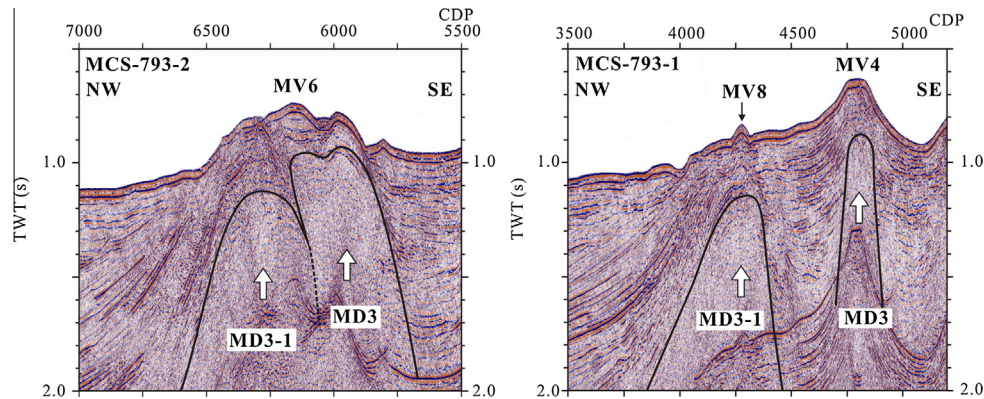
Fig. 8. The development of the mud diapirs MD3 and MD3-1 in MCS profiles of MCS-793-2 and 793-1. Mud diapirs MD3 and MD3-1 can be identified in MCS-793-2 profile and developed as isolated diapiric structures northward to MCS-793-1 profile. See the profiles location in Fig. 3.

Table 1
Locations and characteristics of the mud volcanoes in the near shore of SW Taiwan.

Mud volcano	Coordinates		Water depth	Edifice slope	Size
	Latitude (N)	Longitude (E)			
MV1	N: 22° 9.4939′	E: 120° 23.2667′	365 m	9°	About 95 m high and 1250 m diameter at base
MV2	N: 22° 9.5433′	E: 120° 22.3467′	425 m	12°	About 600 m wide, 1200 m long and 85 m high
MV3	N: 22° 9.5433′	E: 120° 20.2867′	465 m	8°	About 145 m high and 2000 m diameter
MV4	N: 22° 8.6017′	E: 120° 19.4′	465 m	10°	About 140 m high and 1900 m diameter at base
MV5	N: 22° 8.247′	E: 120° 18.6′	430 m	8.6°	About 175 m high and 2200 m diameter at base
MV6	N: 22° 7.3396′	E: 120° 17.3867′	515 m	7.4°	About 135 m high, 2900 m long and 1300 m wide
MV7	N: 22° 10.7248′	E: 120° 18.9334′	540 m	7.2°	About 65 m high and 1100 m diameter at base
MV8	N: 22° 9.7594′	E: 120° 17.9534′	610 m	12.7°	About 75 m high and 680 m diameter at base
MV9	N: 22° 4.889′	E: 120° 14.4271′	610 m	9.5°	About 240 m high and 2800 m diameter at base
MV10	N: 22° 3.537′	E: 120° 15.38′	505 m	13.6°	About 345 m high and 3300 m diameter at base.
MV11	N: 21° 59.8951′	E: 120° 20.42′	760 m	10°	About 240 m high and 3000 m diameter at base
MV12	N: 21° 49.6527′	E: 120° 33.3729′	370 m	9.6°	About 280 m high and 4100 m diameter at base
MV13	N: 21° 46.907′	E: 120° 24.3356′	635 m	5.3°	About 115 m high, 4000 m long and 2500 m wide

(Yang et al., 2011; Hsu et al., 2013b). The gas seeps, gas plumes, pockmarks and active mud volcanoes have been found, indicating that gas-bearing fluids are discharged in the study area (Chen et al., 2010, 2012; Hsu et al., 2013b). The discharge of the gas-bearing fluids is actively modulated by ocean tides (Hsu et al., 2013b). Therefore, we propose the gas-charged sediments play an important role in supporting the diapirism in the study area.

As a result, we suggest that the mechanisms contributing to the formation of the mud diapirs and mud volcanoes are not only due to the existence of overpressure layers and tectonic compressional forces but also due to the gas-bearing fluids in the offshore SW Taiwan. The presence of gas-bearing fluids is also indicated in lower slope domain by the high methane concentrations in both cored sediments (Chuang et al., 2006, 2010, 2013; Lim et al., 2011) and water column samples (Yang et al., 2006). However, the lower slope is characterized by a series of thrusts and folds (Liu et al., 2004; Lin et al., 2008) in contrast to the mud diapirism and mud volcanism in the upper slope domain. Widely distributed BSRs have been observed in the offshore area of SW Taiwan (Liu et al., 2006), indicating the presence of gas hydrate in sedimentary layers. In general, the BSRs are distributed at water depths greater than ∼600 m, including lower slope and part of upper slope areas (Fig. 1). In the upper slope domain, the shallow water depth is unfavorable for the gas hydrate formation. The gas-bearing fluids migrates upwards to support the mud diapirism and volcanism. In contrast, in the lower slope domain where gas hydrate stability conditions are satisfied, the gas-bearing fluids forms gas hydrate in sediment.

In our study area, the gas source is characterized by a mixture of thermogenic and biogenic gases (Yang et al., 2012), found in the Fangliao Ridge (MD8) and in the north end of MD5 areas, implying the mud diapir is an efficient pathway for the vertical migration of thermogenic gas fluid from the deeper part of the sedimentary layers.

5.2. Mud volcano characters

In the study area, the mud volcanoes located on tops of the mud diapirs. The morphology of mud volcanoes could reflect the evolution history (Limonov et al., 1997; Krastel et al., 2003). The key factors are the viscosity of flows and the permeability of feeder (Krastel et al., 2003). The shape of a mud volcano is closely related to the viscosity of the flows. The high viscosity of flows causes a dome-like cone with a steep slope (Shih, 1967; León et al., 2007). Our results show that the slopes of the mud volcanoes are very steep (from 5.3° to 13.6°). We suggest that the mud volcanoes are fed by high-viscosity flows. The 10 mud volcanoes (except the mud volcanoes MV8, MV11 and MV12) with steep cone-shaped craters could be produced by higher viscous flows (Fig. 3) (León et al., 2007). However, 3 mud volcanoes (MV8, MV11 and MV12) could be fed by relative lower-viscosity flows, resulting in the flat volcanic edifice on the crest (Fig. 3).

In terms of size, the mud volcanoes MV9–MV13 (diameters of 2800–4100 m) located at deeper water depths are rather large than the other MV1–MV8 (diameters of 680–2200 m) located at shallower water depths. In general, the fluid migrates gradually from
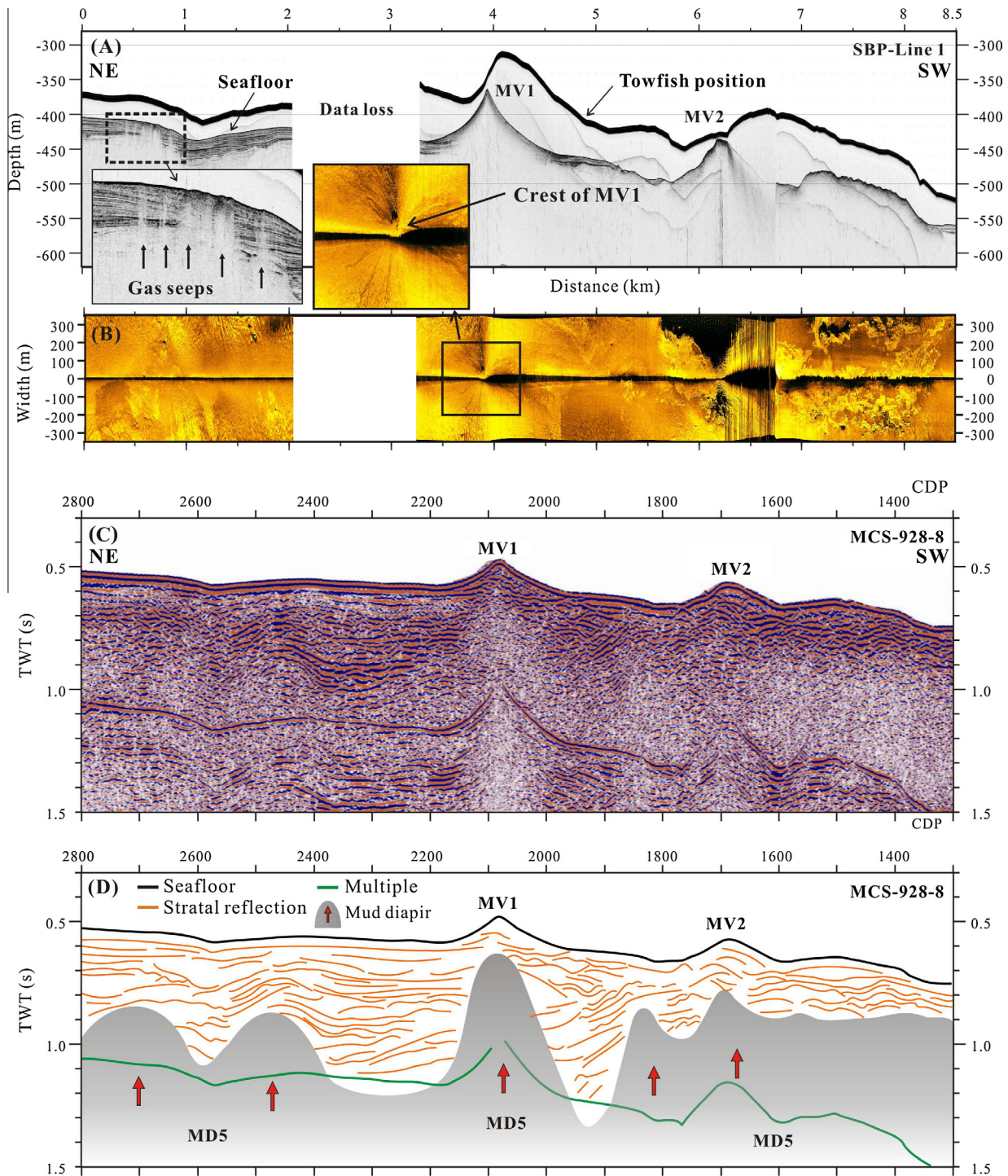
Fig. 9. (A) Sub-bottom profiler image and (B) sidescan sonar image of SBP-line 1, (C) corresponding seismic reflection profile and (D) the interpreted seismic profile of MCS-928-8. See the profiles location in Fig. 3. The radial high backscatter intensity stripes (light tones) are observed on the flank of the mud volcano MV1. The high backscatter intensity is also observed on the flank of mud volcano MV2, south area of mud volcano MV2 and in the center of the volcanoes MV1 and MV2.

deep to shallow water depths, the mud volcanoes located at deeper water depths may have formed earlier than the mud volcanoes at shallower water depths. In this study, we suggest that the large mud volcanoes could be associated with the longer eruption history. The large cone-shaped mud volcano is probably related to high permeability conduits that allow more effusive eruptions (Krastel et al., 2003). The long eruption history could also be as one of the reasons to large mud volcano. However, the high

permeability conduit still cannot be excluded as the reason to form a large mud volcano in the study area.

5.3. Mud diapir controls morphological evolution

The morphology of the upper Kaoping Slope is mainly controlled by the development of mud diapirs. The mud diapiric intrusions resulting in a series of structural highs (Figs. 4–7) and three
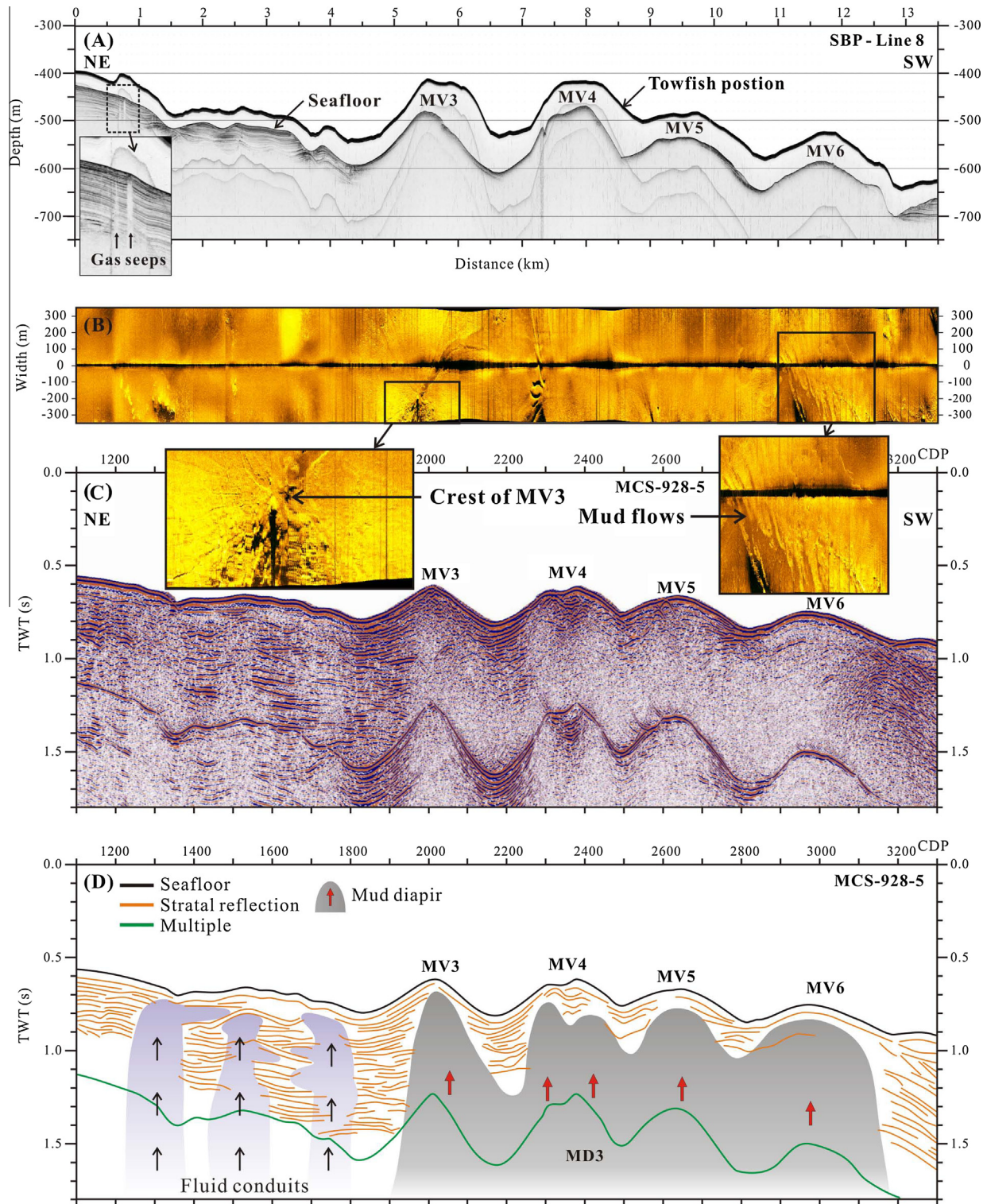
Fig. 10. (A) Sub-bottom profiler image and (B) sidescan sonar image of SBP-line 8, (C) corresponding seismic reflection profile and (D) the interpreted seismic profile of MCS-928-5. See the profiles location in Fig. 3. Note the fluid conduits are observed in the MCS profile and the gas seeps also exist in the sub-bottom profiler. The radial high backscatter intensity stripes (light tones) are observed on the flank of mud volcanoes MV3 and MV6. The high backscatter intensity spot is also observed in the center of mud volcano MV3.

slope basins (SB1–SB3; Figs. 2 and 4–6) are formed between the structural highs. The basins developed are mainly affected by the competition between uplifting of mud diapirs and sedimentary processes (Hsu et al., 2013a). The courses of Kaoping Canyon and Fangliao Canyon are controlled by mud diapiric intrusions. Due

to the uplifting of diapirs the canyon courses are constrained to develop along the flanks of structural highs. The Kaoping Canyon located between the mud diapirs MD1 and MD2 in the north of N22°18′, in the west of MD1 between the N22°18′ and N22°04′, and in the south ends of MD1, MD3 and MD6 to the south of
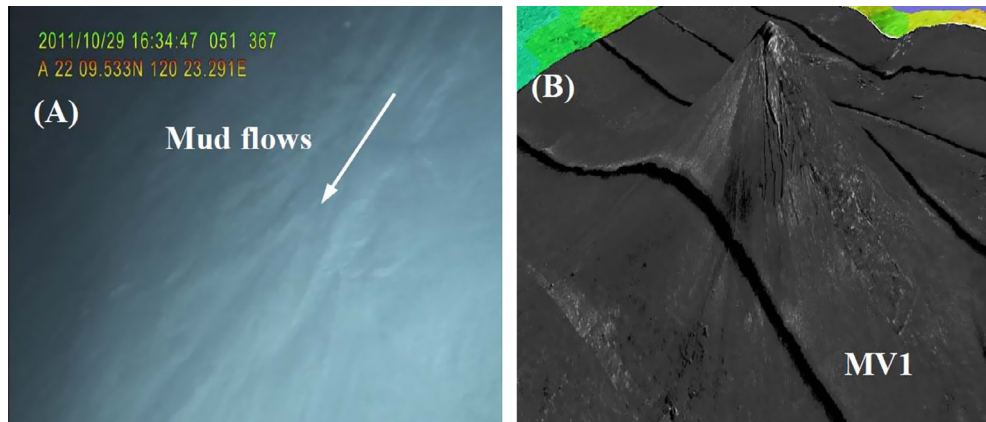
Fig. 11. The mud flows out of the mud volcano MV1. (A) The photo of mud flows on the flank of mud volcano MV1 taken by ROV (Chen et al., 2012). (B) Mosaic image of the deep-towed sidescan sonar data in the mud volcano MV1 area where mud flows edifice is observed.

N22°04′ (Fig. 2). The Fangliao Canyon is an incised valley within slope basin (SB3) (Fig. 5; Hsu et al., 2013a), indicating that it is formed after mud diapiric intrusions. The head of Fangliao Canyon located between the mud diapirs MD7 and MD9 in the north of MD8 (~N22°09′) and the canyon course is shifted to the west of MD8 to the south of N22°09′ due to the obstruction of structural high MD8 on the course way (Fig. 2). We suggest that the courses and morphologies of the Kaoping Canyon and Fangliao Canyon are strongly dominated by mud diapiric intrusions.

6. Conclusions

(1) We have examined ~1500 km long MCS profiles off SW Taiwan and identified the distribution of the ten mud diapirs oriented NNE–SSW to N–S.

(2) Most of the diapiric structures are covered by young sediments, but some have pierced through thick sediments and are exposed at the seafloor. Examples include the Shell-Tomb Ridge, the south pinnacle of MD5, the Fangliao Ridge (MD8) and Xiaoliuchiu islet (MD2). The disturbance of sedimentary strata on both sides and top of the diapiric structures suggests the diapirism is active. However, MD10 is probably inactive because the sedimentary strata deposited above the diapir are undisturbed.

(3) For the first time, 13 mud volcanoes are clearly identified on the basis of the multibeam bathymetric data in the near shore area of SW Taiwan. The distribution of the mud volcanoes is closely associated with the mud diapirs, as they are located on tops of the diapiric structures. The cone-shaped mud volcanoes with steep slopes of 5.3–13.6° indicate a vigorous upward flux of free gas.

(4) The large cone-shaped mud volcanoes located at deeper water depths could be related to the longer eruption history.

(5) Except for mud volcanoes MV8, MV11, MV12, most mud volcanoes show steep cone-shaped craters that are attributed to higher viscous flows. Mud volcanoes MV8, MV11, MV12 could be fed by relatively low viscosity flows because of the flat edifice on the crest. The mud flows on the flank of mud volcanoes MV1, MV3 and MV6 are characterized by radial high backscatter intensity on the sidescan sonar images.

(6) The formation of mud diapirs and mud volcanoes off SW Taiwan can be controlled by three factors: (i) the overpressure in sedimentary layers, caused by rapid sedimentation rates; (ii) the mud diapirism, triggered by the convergent stress between the Philippine Sea Plate and the Eurasian Plate; and (iii) the upward migration of the gas-bearing fluids with decreasing mud densities and increasing buoyancy forces.

(7) The morphology of the upper Kaoping Slope is mainly controlled by mud diapiric intrusions. The slope basins are formed between structural highs (mud diapirs). The courses of Kaoping Canyon and Fangliao Canyon have developed along the flanks of a diapir or between diapirs.

References

Bangs, N.L.B., Musgrave, R.J., Tréhu, A.M., 2005. Upward shifts in the southern Hydrate Ridge gas hydrate stability zone following postglacial warming, offshore Oregon. Journal of Geophysical Research 110 (B03102), 1–13.

Bowin, C., Ru, R.-S., Lee, C.-S., Schouten, H., 1978. Plate convergence and accretion in Taiwan-Luzon regions. American Association of Petroleum Geologists Bulletin 62, 1645–1672.

Brown, K.M., 1990. The nature and hydrogeologic significance of mud diapirs and diatremes for accretionary systems. Journal of Geophysical Research 95 (B6), 8969–8982.

Brown, K., Westbrook, G.K., 1988. Mud diapirism and subcretion in the Barbados Ridge accretionary complex: the role of fluids in accretionary processes. Tectonics 7 (3), 613–640.

Camerlenghi, A., Cita, M.B., Della Vedova, B., Fusi, N., Mirabile, L., Pellis, G., 1995. Geophysical evidence of mud diapirism on the Mediterranean Ridge accretionary complex. Marine Geophysical Research 17, 115–141.

Chang, C.-H., 1993. Mud diapirs in offshore Southwestern Taiwan. Thesis, Institute of Oceanography, National Taiwan University, Taiwan, p. 71 (in Chinese).

Chen, S.-C., Hsu, S.-K., Tsai, C.-H., Ku, C.-Y., Yeh, Y.-C., Wang, Y., 2010. Gas seepage, pockmarks and mud volcanoes in the near shore of SW Taiwan. Marine Geophysical Research 31, 133–147.

Chen, S.-C., Hsu, S.-K., Tsai, C.-H., Wang, Y., Chung, S.-H., Chen, P.-C., Liu, C.-S., Yang, T.F., 2012. Active mud volcanoes and gas seeps in the near shore of SW Taiwan. In: 11th International conference on gas in marine sediments, 4–7 September 2012, Nice, France, Program and abstracts, 99.

Chi, W.-R., 1981. Calcareous nannoplankton from the sediments of the Liuchiuhsu, southwestern Taiwan. Proceedings of the Geological Society of China 24, 141–147.

Chiang, C.-S., Yu, H.-S., 2006. Morphotectonics and incision of the Kaoping submarine canyon, SW Taiwan orogenic wedge. Geomorphology 80, 199–213.

Chiu, J.-K., Tseng, W.-H., Liu, C.-S., 2006. Distribution of gassy sediments and mud volcanoes offshore southwestern Taiwan. Terrestrial, Atmospheric and Oceanic Sciences 17, 703–722.

Chuang, H.-J., 2006. Distribution and structural relationships of mud diapirs offshore southwestern Taiwan. Thesis, Institute of Oceanography, National Taiwan University, Taiwan, p. 113 (in Chinese).

Chuang, P.-C., Dale, A.W., Wallmann, K., Haeckel, M., Yang, T.F., Chen, N.-C., Chen, H.-C., Chen, H.-W., Lin, S., Sun, C.-H., You, C.-F., Horng, C.-S., Wang, Y., Chung, S.-H., 2013. Relating sulfate and methane dynamics to geology: the accretionary prism offshore SW Taiwan. Geochemistry, Geophysics, Geosystems 4, 2523–2545.

Chuang, P.-C., Yang, T.F., Hong, W.-L., Lin, S., Sun, C.-H., Lin, A.T., Chen, J.-C., Wang, Y., Chung, S.-H., 2010. Estimation of methane flux offshore SW Taiwan and the influence of tectonics on gas hydrate accumulation. Geofluids 10, 497–510.

Chuang, P.-C., Yang, T.F., Lin, S., Lee, H.-F., Lan, T.-F., Hong, W.-L., Liu, C.-S., Chen, J.-C., Wang, Y., 2006. Extremely high methane concentration in bottom water and cored sediments from offshore southwestern Taiwan. Terrestrial, Atmospheric and Oceanic Sciences 17, 903–920.

Dadson, S.J., Hovius, N., Chen, H., Dade, W.B., Hsieh, M.-L., Willett, S.D., Hu, J.-C., Horng, M.-J., Chen, M.-C., Stark, C.P., Laque, D., Lin, J.-C., 2003. Links between erosion, runoff variability and seismicity in the Taiwan orogen. Nature 426, 648–651.

Dimitrov, L.I., 2002. Mud volcanoes—the most important pathway for degassing deeply buried sediments. Earth-Science Reviews 59, 49–76.

Dimitrov, L.I., 2003. Mud volcanoes—a significant source of atmospheric methane. Geo-Marine Letters 23, 155–161.

Gamberi, F., Rovere, M., 2010. Mud diapirs, mud volcanoes and fluid flow in the rear of the Calabrian Arc Orogenic Wedge (southeastern Tyrrhenian sea). Basin Research 22, 452–464.

Hale, R.P., Nittrouer, C.A., Liu, J.T., Keil, R.G., Ogston, A.S., 2012. Effects of a major typhoon on sediment accumulation in Fangliao Submarine Canyon, SW Taiwan. Marine Geology 326–328, 116–130.

Ho, C.-S., 1986. A synthesis of the geological evolution of Taiwan. Tectonophysics 125, 1–16.

Holbrook, W.S., Hoskins, H., Wood, W.T., Stephen, R.A., Lizzarralde, D., the Leg 164 Science Party, 1996. Methane hydrate and free gas on the Blake Ridge from vertical seismic profiling. Science 273, 1840–1843.

Holland, C.W., Weber, T.C., Etiope, G., 2006. Acoustic scattering from mud volcanoes and carbonate mounds. Journal of the Acoustical Society of America 120 (6), 3553–3565.

Hovland, M., Curzi, P.V., 1989. Gas seepage and assumed mud diapirism in the Italian central Adriatic Sea. Marine and Petroleum Geology 6, 161–169.

Hovland, M., Hill, A., Stokes, D., 1997. The structure and geomorphology of the Dashgil mud volcano, Azerbaijan. Geomorphology 21, 1–15.

Hsieh, S.-H., 1970. Geology and gravity anomalies of the Pingtung Plain, Taiwan. Proceedings of the Geological Society of China 13, 76–89.

Hsu, H.-H., Liu, C.-S., Yu, H.-S., Chang, J.-H., Chen, S.-C., 2013a. Sediment dispersal and accumulation in tectonic accommodation across the Gaoping Slope, offshore Southwestern Taiwan. Journal of Asian Earth Sciences 69, 26–38.

Hsu, S.-K., Wang, S.-Y., Liao, Y.-C., Yang, T.F., Jan, S., Lin, J.-Y., Chen, S.-C., 2013b. Tide-modulated gas emissions and tremors off SW Taiwan. Earth and Planetary Science Letters 369–370, 98–107.

Huang, W.-L., 1995. Distribution and mud diapirs offshore southwestern Taiwan, their relations to the onland anticlinal structures and their effectson the deposition environment in southwestern Taiwan. Thesis, Institute of Oceanography, National Taiwan University, Taiwan, p. 68 (in Chinese).

Huh, C.-A., Lin, H.-L., Lin, S., Huang, Y.-W., 2009. Modern accumulation rates and a budget of sediment off the Gaoping (Kaoping) River, SW Taiwan: a tidal and flood dominated depositional environment around a submarine canyon. Journal of Marine Systems 76, 405–416.

Hyndman, R.D., Dallimore, S.R., 2001. Natural gas hydrate studies in Canada. Canadian Society of Exploration Geophysicists, Recorder 26 (5), 11–20.

Johnson, J.E., Goldfinger, C., Suess, E., 2003. Geophysical constraints on the surface distribution of authigenic carbonates across the Hydrate Ridge region, Cascadia margin. Marine Geology 202 (1), 79–120.

Kobayashi, K., Ashi, J., Boulegue, J., Cambray, H., Chamot-Rooke, N., Fujimoto, H., Furuta, T., Iiyama, J.T., Koizumi, T., Mitsuzawa, K., Monma, H., Murayama, M., Naka, J., Nakanishi, M., Ogawa, Y., Otsuka, K., Okada, M., Oshida, A., Shima, N., Soh, W., Takeuchi, A., Watanabe, M., Yamagata, T., 1992. Deep-tow survey in the KAIKO-Nankai cold seepage areas. Earth and Planetary Science Letters 109, 347–354.

Kopf, A.J., 2002. Significance of mud volcanism. Review of Geophysics 40 (2), 1–52.

Kopf, A., Robertson, A.H.F., Clennell, M.B., Flecker, R., 1998. Mechanism of mud extrusion on the Mediterranean Ridge accretionary complex. Geo-Marine Letters 18, 97–114.

Kopf, A., Robertson, A.H.F., Volkmann, N., 2000. Origin of mud breccia from the Mediterranean Ridge accretionary complex based on evidence of the maturity of organic matter and related petrographic and regional tectonic evidence. Marine Geology 166, 65–82.

Krastel, S., Spiess, V., Ivanov, M., Weinrebe, W., Bohrmann, G., Shashkin, P., Heidersdorf, F., 2003. Acoustic investigations of mud volcanoes in the Sorokin Trough, Black Sea. Geo-Marine Letters 23, 230–238.

Lacombe, O., Angelier, J., Mouthereau, F., Chu, H.-T., Deffontaines, B., Lee, J.-C., Rocher, M., Chen, R.-F., Siame, L., 2004. The Liuchiu Hsu island offshore SW Taiwan: tectonic versus diapiric anticline development and comparisons with onshore structures. Comptes Rendus Geoscience 336, 815–825.

León, R., Somoza, L., Medialdea, T., González, F.J., Díaz-del-Río, V., Fernández-Puga, M.C., Maestro, A., Mata, M.P., 2007. Sea-floor features related to hydrocarbon seeps in deepwater carbonate-mud mounds of the Gulf of Cádiz: from mud flows to carbonate precipitates. Geo-Marine Letters 27, 237–247.

Lim, Y.-C., Lin, S., Yang, T.F., Chen, Y.-G., Liu, C.-S., 2011. Variations of methane induced pyrite formation in the accretionary wedge sediments offshore southwestern Taiwan. Marine and Petroleum Geology 28, 1829–1837.

Limonov, A.F., van Weering, Tj.C.E., Kenyon, N.H., Ivanov, M.K., Meisner, L.B., 1997. Seabed morphology and gas venting in the Black Sea mudvolcano area: observations with the MAK-1 deep-tow sidescan sonar and bottom profiler. Marine Geology 137, 121–136.

Limonov, A.F., Woodside, J.M., Cita, M.B., Ivanov, M.K., 1996. The Mediterranean Ridge and related mud diapirism: a background. Marine Geology 132, 7–19.

Lin, A.T., Liu, C.-S., Lin, C.-C., Schnürle, P., Chen, G.-Y., Liao, W.-Z., Teng, L.S., Chuang, H.-J., Wu, M.-S., 2008. Tectonic features associated with the overriding of an accretionary wedge on top of a rifted continental margin: an example from Taiwan. Marine Geology 255, 186–203.

Lin, A.T., Yao, B., Hsu, S.-K., Liu, C.-S., Huang, C.-Y., 2009. Tectonic features of the incipient arc-continent collision zone of Taiwan: implications for seismicity. Tectonophysics 479, 28–42.

Lin, C.-C., Lin, A.T., Liu, C.-S., Horng, C.-S., Chen, G.-Y., Wang, Y., 2013. Canyon-infilling and gas hydrate occurrences in the frontal fold of the offshore accretionary wedge off southern Taiwan, Marine Geophysical Research. http://dx.doi.org/10.1007/s11001-013-9203-7.

Liu, C.-S., Huang, I.-L., Teng, L.S., 1997. Structural features off southwestern Taiwan. Marine Geology 137, 305–319.

Liu, C.-S., Deffontaines, B., Lu, C.-Y., Lallemand, S., 2004. Deformation patterns of an accretionary wedge in the transition zone from subduction to collision offshore southwestern Taiwan. Marine Geophysical Research 25, 123–137.

Liu, C.-S., Schnürle, P., Wang, Y., Chung, S.-H., Chen, S.-C., Hsiuan, T.-H., 2006. Distribution and characters of gas hydrate offshore of southwestern Taiwan. Terrestrial, Atmospheric and Oceanic Sciences 17, 615–644.

Milkov, A.V., 2000. Worldwide distribution of submarine mud volcanoes and associated gas hydrates. Marine Geology 167, 29–42.

Morita, S., Ashi, J., Aoike, K., Kuramoto, S., 2004. Evolution of Kumano basin and sources of clastic ejecta and pore fluid in Kumano mud volcanoes, Eastern Nanaki Trough. In: Proceedings of the International Symposium on Methane Hydrates and Fluid Flow in Upper Accretionary Prisms, Engineering Geology Laboratory. Department of Civil & Earth Resources Engineering, Kyoto University, Kyoto, pp. 92–99.

Naudts, L., Greinert, J., Artemov, Y., Beaubien, S.E., Borowski, C., De Batist, M., 2008. Anomalous sea-floor backscatter patterns in methane venting areas, Dnepr paleo-delta, NW Black Sea. Marine Geology 251, 253–267.

Orange, D.L., Yun, J., Maher, N., Barry, J., Greene, G., 2002. Tracking California seafloor seeps with bathymetry, backscatter and ROVs. Continental Shelf Research 22, 2273–2290.

Pérez-Belzuz, F., Alonso, B., Ercilla, G., 1997. History of mud diapirism and trigger mechanisms in the Western Alboran Sea. Tectonophysics 282, 399–422.

Reed, D.L., Lundberg, N., Liu, C.-S., Kuo, B.-Y., 1992. Structural relations along the margins of the offshore Taiwan accretionary wedge: implications for accretion and crustal kinematics. Acta Geologica Taiwanica 30, 105–122.

Robertson, A., Ocean Drilling Program Leg 160 Scientific Party, 1996. Mud volcanism on the Mediterranean Ridge: Initial Results of Ocean Drilling Program Leg 160. Geology 24 (3), 239–242.

Sautkin, A., Talukder, A.R., Comas, M.C., Soto, J.I., Alekseev, A., 2003. Mud volcanoes in the Alboran Sea: evidence from micropaleontological and geophysical data. Marine Geology 195, 237–261.

Shih, T.-T., 1967. A survey of the active mud volcanoes in Taiwan and a study of their types and the character of the mud. Petroleum Geology of Taiwan 5, 259–311.

Somoza, L., Díaz-del-Río, V., León, R., Ivanov, M., Fernández-Puga, M.C., Gardner, J.M., Hernández-Molina, F.J., Pinheiro, L.M., Rodero, J., Lobato, A., Maestro, A., Vázquez, J.T., Medialdea, T., Fernández-Salas, L.M., 2003. Seabed morphology and hydrocarbon seepage in the Gulf of Cádiz mud volcano area: acoustic imagery, multibeam and ultra-high resolution seismic data. Marine Geology 195, 153–176.

Sumner, R.H., Westbrook, G.K., 2001. Mud diapirism in front of the Barbados accretionary wedge: the influence of fracture zones and North American–South American plate motions. Marine and Petroleum Geology 18, 591–613.

Sun, C.-H., Chang, S.-C., Kuo, C.-L., Wu, J.-C., Shao, P.-H., Oung, J.-N., 2010. Origins of Taiwan's mud volcanoes: evidence from geochemistry. Journal of Asian Earth Sciences 37, 105–116.

Sun, S.-C., Liu, C.-S., 1993. Mud diapir and submarine channel deposits in offshore Kaosiung-Hengchun, southwest Taiwan. Petroleum Geology of Taiwan 28, 1–14.

Talukder, A.R., Bialas, J., Klaeschen, D., Buerk, D., Brueckmann, W., Reston, T., Breitzke, M., 2007. High-resolution, deep tow, multichannel seismic and sidescan sonar survey of the submarine mounds and associated BSR off Nicaragua pacific margin. Marine Geology 241, 33–43.

Talukder, A.R., Comas, M.C., Soto, J.I., 2003. Pliocene to Recent mud diapirism and related mud volcanoes in the Alboran Sea (Western Mediterranean). Geological Society, London, Special Publications 216, 443–459.

Teng, L.S., 1990. Geotectonic evolution of late Cenozoic arc-continent collision in Taiwan. Tectonophysics 183, 57–76.

Tseng, W.-H., 2006. Distribution and mechanism of submarine mud volcanoes offshore southwestern Taiwan. Thesis, Institute of Oceanography, National Taiwan University, Taiwan, p. 62 (in Chinese).

Yang, T.F., Chen, N.-C., Chuang, P.-C., Chen, C.-W., Lin, S., Sun, C.-H., Chung, S.-H., Wang, Y., 2011. Gas sources of gas hydrate potential area offshore SW Taiwan. 2011 conference on gas hydrate investigations, 20 October 2011, Taipei, Taiwan, Program and abstracts, 16–19 (in Chinese).

Yang, T.F., Chuang, P.-C., Chen, C.-W., Chen, N.-C., Lin, S., Wang, Y., Chung, S.-H., Chen, P.-C., 2012. Gas composition of cored sediments from gas hydrate potential area offshore SW Taiwan. In: 11th international conference on gas in marine sediments, 4–7 September 2012, Nice, France, Program and abstracts, 91.

Yang, T.F., Chuang, P.-C., Lin, S., Chen, J.-C., Wang, Y., Chung, S.-H., 2006. Methane venting in gas hydrate potential area offshore of SW Taiwan: evidence of gas analysis of water column samples. Terrestrial, Atmospheric and Oceanic Sciences 17, 933–950.

Yang, T.F., Yeh, G.-H., Fu, C.-C., Wang, C.-C., Lan, T.-F., Lee, H.-F., Chen, C.-H., Walia, V., Sung, Q.-C., 2004. Composition and exhalation flux of gases from mud volcanoes in Taiwan. Environmental Geology 46, 1003–1011.

Yeh, G.-H., 2003. Geochemistry and sources of mud-volcano fluids in Taiwan. Thesis, Institute of Oceanography, National Taiwan University, Taiwan, p. 61 (in Chinese).

Yu, H.-S., Chiang, C.-S., Shen, S.-M., 2009. Tectonically active sediment dispersal system in SW Taiwan margin with emphasis on the Gaoping (Kaoping) Submarine Canyon. Journal of Marine Systems 76, 369–382.